Production of a beam of highly vibrationally excited CO using perturbations

Nils Bartels, Tim Schäfer, Jens Hühnert, Robert W. Field, and Alec M. Wodtke

Citation: J. Chem. Phys. **136**, 214201 (2012); doi: 10.1063/1.4722090
View online: http://dx.doi.org/10.1063/1.4722090
View Table of Contents: http://jcp.aip.org/resource/1/JCPSA6/v136/i21
Published by the American Institute of Physics.

Additional information on J. Chem. Phys.

Journal Homepage: http://jcp.aip.org/
Journal Information: http://jcp.aip.org/about/about_the_journal
Top downloads: http://jcp.aip.org/features/most_downloaded
Information for Authors: http://jcp.aip.org/authors

ADVERTISEMENT

Downloaded 02 Jul 2012 to 134.76.223.56. Redistribution subject to AIP license or copyright; see http://jcp.aip.org/about/rights_and_permissions

Production of a beam of highly vibrationally excited CO using perturbations

Nils Bartels,[1] Tim Schäfer,[1] Jens Hühnert,[1] Robert W. Field,[2] and Alec M. Wodtke[1,3,a)]
[1]*Institute for Physical Chemistry, Georg August University of Göttingen, Tammanstraße 6, 37077 Göttingen, Germany*
[2]*Massachusetts Institute of Technology, 77 Massachusetts Avenue, Room 6-219, Cambridge, Massachusetts 02139, USA*
[3]*Max Planck Institute for Biophysical Chemistry, Department of Dynamics at Surfaces, Am Faßberg 11, 37077 Göttingen, Germany*

(Received 5 April 2012; accepted 9 May 2012; published online 5 June 2012)

An intense molecular beam of CO ($X^1\Sigma^+$) in high vibrational states ($v = 17, 18$) was produced by a new approach that we call *PUMP – PUMP – PERTURB* and *DUMP*. The basic idea is to access high vibrational states of CO $e^3\Sigma^-$ via a two-photon doubly resonant transition that is perturbed by the $A^1\Pi$ state. *DUMP* -ing from this mixed (predominantly triplet) state allows access to high vibrational levels of CO ($X^1\Sigma^+$). The success of the approach, which avoids the use of vacuum UV radiation in any of the excitation steps, is proven by laser induced fluorescence and resonance enhanced multi-photon ionization spectroscopy. © *2012 American Institute of Physics*. [http://dx.doi.org/10.1063/1.4722090]

INTRODUCTION

Molecular beam scattering in combination with high resolution spectroscopy is a key experimental technique for studying quantum-state resolved chemical reactivity.[1–4] Since the development of stimulated emission pumping (SEP),[5,6] it has also become feasible to study the behavior of molecules selectively prepared in high vibrational states, carrying several eV of internal energy. SEP spectroscopy has been proven applicable to a wide variety of molecules. These include: I_2,[5] C_2H_2,[7] CH_2O,[8] NO,[9,10] HCN,[11,12] H(or D)FCO,[13,14] HCP,[15,16] Tropolone,[17,18] CS_2,[19,20] SO_2,[21] $SCCl_2$,[22] CH_3O,[23] HCO,[24] and O_2.[25,26] See Refs. 6 and 27 for detailed information.

The use of SEP to prepare sufficient population of highly vibrationally excited molecules to carry out collision experiments has so far been limited to a much smaller number of molecules: O_2, NO, and CH_2O.

NO is one example that has been particularly important for studies of vibrational energy transfer in collisions of highly vibrationally excited molecules at a solid surface[28–32] and in the gas phase.[10] Such experiments have, for example, led to clear evidence of electronically nonadiabatic interactions – breakdown of the Born Oppenheimer approximation– in collisions of NO($v \gg 0$) with a metal surface.[33–38]

To be able to carry out similar experiments on a wider variety of molecules, we have been developing alternative means of optically pumping small molecules to high vibrational states, for example, using overtone pumping.[39,40] Despite these successes, better methods are clearly needed. Of the many small molecules that could be candidates for study, CO is one of the most attractive and heavily studied within the context of molecule–surface interactions.[41,42] However, up to now, the $X^1\Sigma^+$ state of CO has only been pumped to high vibrational states by energy pooling upon IR irradiation[43,44] or by electron impact desorption from transition metal surfaces.[45] Both of these methods are impractical approaches to *state specific* preparation of CO for scattering experiments. In this work, we present an approach to the production of highly vibrationally excited CO using an optical pumping scheme that is very similar to SEP, which we now describe.

The method relies on the strong transition strength of the CO 4th-positive system $A^1\Pi_1 \leftarrow X^1\Sigma^+$, whose electronic oscillator strengths have been reported.[46] In principle, this is an absorption system that could be used for conventional SEP. Unfortunately, this band lies deep in the vacuum ultraviolet where intense laser light sources are difficult to implement or entirely unavailable. In *PUMP – PUMP – PERTURB* and *DUMP* (P^3D), $A^1\Pi_1$ is reached via a two-step transition through the triplet manifold, relying on molecular spin-orbit perturbations. Figure 1 shows how the large oscillator strength of the 4th-positive system $A^1\Pi_1 \leftarrow X^1\Sigma^+$,[47] is loaned to the triplet manifold, allowing some nominally spin-forbidden transitions to be exploited for optical pumping. Specifically, spin-orbit mixing between $A^1\Pi_1$ and $a^3\Pi_1$ allows direct access to the triplet manifold via the Cameron bands, $a^3\Pi_1(v' = 0) \leftarrow X^1\Sigma(v'' = 0)$. We hereafter call this transition $PUMP_1$. We then employ ($PUMP_2$) an allowed triplet-triplet transition, $e^3\Sigma^-(v = 12) \leftarrow a^3\Pi_1(v = 0)$, in order to take advantage of accidental resonances at low J that mix $e^3\Sigma^-(v = 12)$ with $A^1\Pi(v = 8)$. This two-photon transition,

$$e^3\Sigma^-(v = 12) \overset{PUMP_2}{\leftarrow} a^3\Pi_1(v = 0) \overset{PUMP_1}{\leftarrow} X^1\Sigma^+(v = 0), \quad (1)$$

provides access to several rotational levels with significant $A^1\Pi_1(v = 8)$ character at an excitation energy of about 75 000 cm^{-1}. This state has favorable Franck-Condon factors with very high vibrational states of $X^1\Sigma^+$. The principle of P^3D could also be applied via other triplet states, as local

a)Author to whom correspondence should be addressed. Electronic mail: alec.wodtke@mpibpc.mpg.de.

 © 2012 American Institute of Physics

Downloaded 02 Jul 2012 to 134.76.223.56. Redistribution subject to AIP license or copyright; see http://jcp.aip.org/about/rights_and_permissions

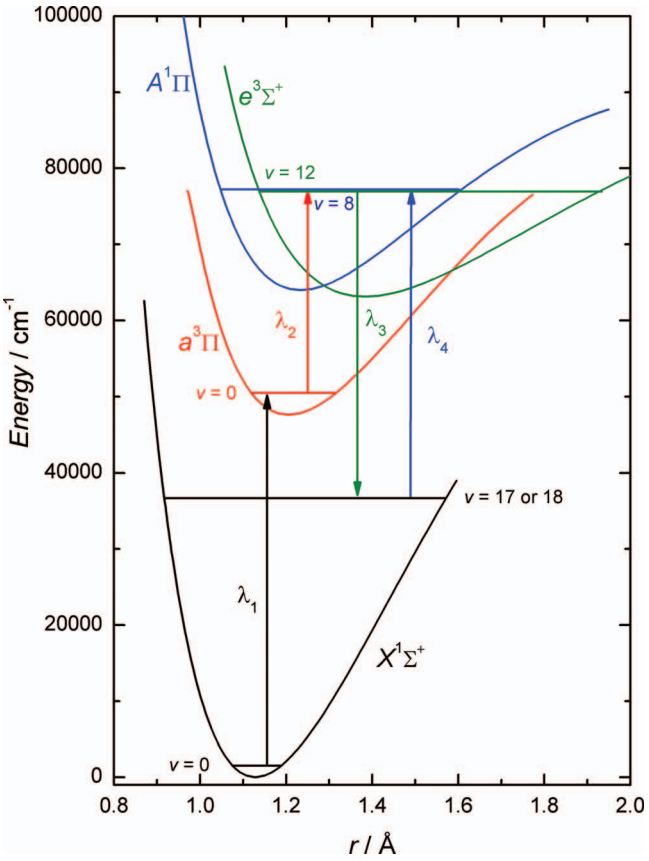

FIG. 1. P^{3}D concept for CO in a potential energy diagram. $PUMP_1(\lambda_1)$ excites to $v = 0$ of the metastable $a^3\Pi$ state (black arrow). From there $PUMP_2(\lambda_2)$ excites to $e^3\Sigma^-(v = 12)$ (red arrow) which is perturbed by the $A^1\Pi_1(v = 8)$ state. At $J = 1$, $e^3\Sigma^-(v = 12)$ lies ~50 cm^{-1} below $A^1\Pi_1(v = 8)$. The perturbation leads efficiently to very high vibrational levels of $X^1\Sigma^+$ ($v \gg 0$) and emission can be enhanced in a $DUMP(\lambda_3)$ step (green arrow). For the $PROBE(\lambda_4)$ step (blue arrow) (1 + 1) REMPI spectroscopy via $A^1\Pi_1(v = 8)$ is performed.

perturbations by the $A^1\Pi_1$ state are ubiquitous. However, the number of perturbations that occur at low J is small. The extent to which other perturbations might be useful in a molecular beam experiment, where the sample rotational temperature is less than 10 K needs to be explored. For experiments to be carried out at higher sample rotational temperatures, many other P^{3}D schemes could be realized. The mixed singlet-triplet character of the $e^3\Sigma^-(v = 12) \sim A^1\Pi_1(v = 8)$ perturbed states used here gives rise to μ s radiative lifetimes, which is also convenient for SEP with ns pulsed lasers. Despite the small singlet character of these perturbed states, the large 4th-positive oscillator strength ensures that a majority of this state's population can be radiatively transferred to $X^1\Sigma^+$. After describing the experiment next, we present results demonstrating v, J–selective stimulated emission to $X^1\Sigma^+(v = 17, 18)$ vibrational states of CO with more than four eV of vibrational energy.

EXPERIMENTAL DETAIL

The experiments are carried out in a molecular beam apparatus similar to that described in previous papers.[48,49] Briefly, a pulsed supersonic molecular beam of rotationally cold CO molecules is produced by expanding mixtures of CO seeded in a carrier gas (20% CO in Kr ($T_{Rot} \sim 10$ K), 20% CO in Ar ($T_{Rot} \sim 5$ K), or 10% CO in H_2 ($T_{Rot} \sim 40$ K)) into vacuum through a piezoelectric valve (1 mm diameter nozzle, 10 Hz, 3 atm stagnation pressure). After passing a 2 mm electro-formed skimmer (Ni Model 2, Beam dynamics, Inc.) 3 cm downstream, the beam enters a differentially pumped region ($p \sim 10^{-7}$ Torr), where the laser beams (9 cm distance from nozzle) used for the $PUMP_1$, $PUMP_2$, and $DUMP$ steps cross the molecular beam, which are all overlapped in time and space. The molecules then pass through an aperture and enter another differentially pumped vacuum chamber ($p \sim 10^{-9}$ Torr), where the population distribution in the $X^1\Sigma^+$ state can be detected in the $PROBE$ step using (1 + 1) resonance enhanced multi-photon ionization (REMPI) spectroscopy (26 cm distance from nozzle).

$PUMP_1$ transitions – See Fig. 1 – can be nearly saturated using a Fourier transform limited UV pulse from a Nd:YAG pumped home-built optical parametric oscillator with sum frequency generation unit (OPO-SFG) laser system at 206 nm,[50] with 1 mJ pulse energy, 200 MHz linewidth, 6 ns pulse length, and 3 mm beam diameter. The $PUMP_2$ step was typically performed with a power of 0.5 mJ/pulse at 368 nm (beam diameter of 5 mm), although the transition was already saturated with 100 μJ/pulse. The $DUMP$ and the $PROBE$ step (~234 nm) were both performed with 1 mJ/pulses with 3 and 5 mm beam diameter for the $DUMP$ and $PROBE$ steps, respectively. In this experiment, all four laser beams were linearly polarized in the z-direction, which is defined as the propagation direction of the molecular beam.

Light for the $PUMP_2$, $DUMP$, and $PROBE$ steps is produced from three frequency doubled dye lasers (Sirah Laser & Plasmatechnik PRSC-DA-24, CSTR-LG-24, and CSTR-DA-24). Each dye laser produces ns pulses with circa 3 GHz bandwidth. Two dye lasers ($DUMP$ and $PROBE$) are themselves each pumped by the 3rd harmonic of a Nd:YAG laser (Continuum PL 7010). The $PUMP_2$ dye laser was pumped by the 2nd harmonic of a third Nd:YAG laser (Spectra Physics Pro 270).

Figure 2 shows a detailed energy diagram describing the optical pumping scheme more concretely. The $PUMP_1$ step produces CO $a^3\Pi_1(v = 0, J = 1)$ via Cameron band excitation,[51] as in previous work.[52,53]

$$a^3\Pi_1(v = 0, J = 1, +, f) \leftarrow X^1\Sigma^+(v = 0, J = 1, -, e)$$
$$\lambda_1 = 206.277 \text{ nm}. \quad (2)$$

Note the wavelengths, λ_i, refer to Fig. 1.

Alternatively, it is possible to excite CO into the (−) parity state.

$$a^3\Pi_1(v = 0, J = 1, -, e) \leftarrow X^1\Sigma^+(v = 0, J = 0, +, e)$$
$$\lambda_1 = 206.293 \text{ nm}. \quad (3)$$

The choice of the starting parity determines the parity after all other steps, as the parity selection rule holds strictly for all optical pumping steps.

Downloaded 02 Jul 2012 to 134.76.223.56. Redistribution subject to AIP license or copyright; see http://jcp.aip.org/about/rights_and_permissions

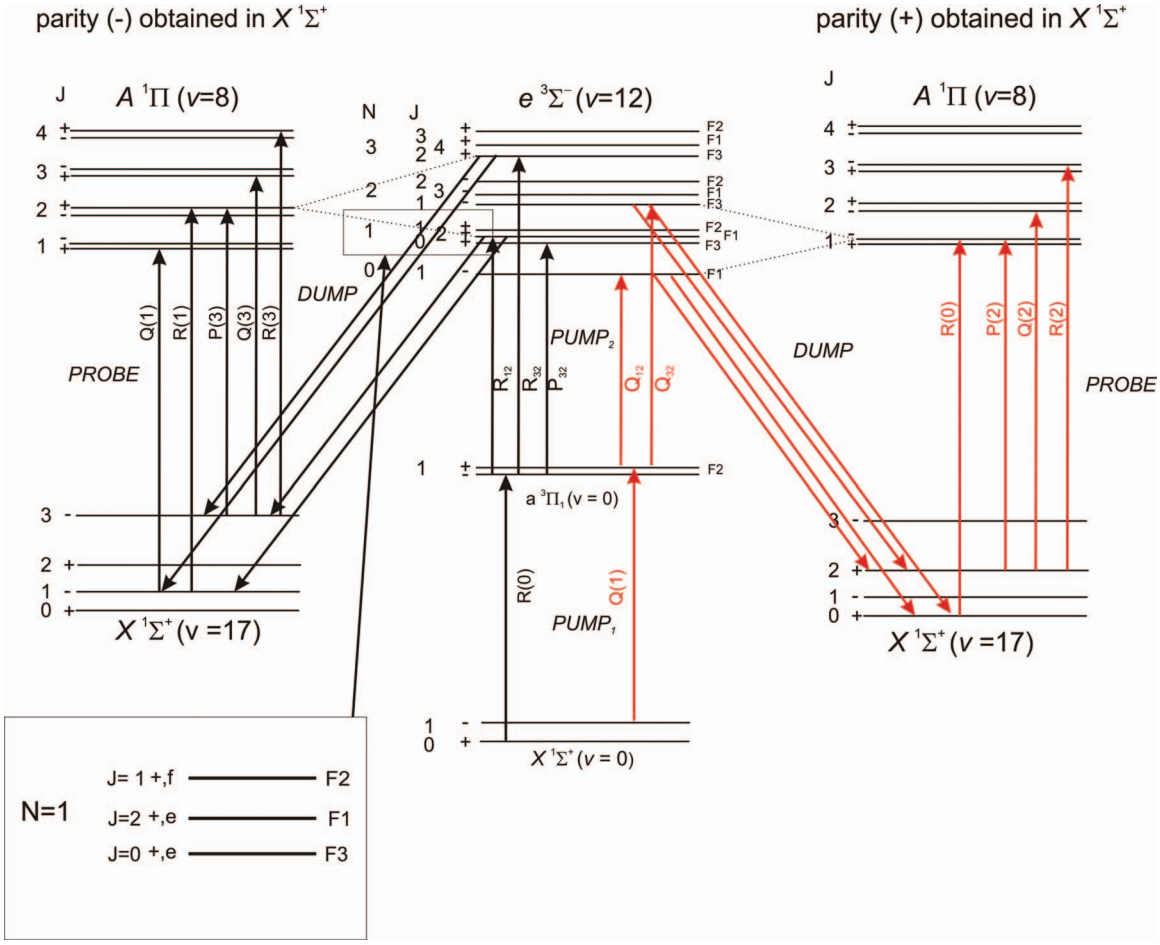

FIG. 2. Energy levels and transitions important for P^3D in CO. In the $PUMP_1(\lambda_1)$ step the $J = 1$ level of $a^3\Pi_1(v = 0)$ can be accessed either in the (+) or in the (−) parity component (via $Q(1)$ or $R(0)$ transition, respectively), which are separated only by the Λ-splitting of ∼0.013 cm^{-1}. $PUMP_2(\lambda_2)$ excites transitions of the $e^3\Sigma^-(v = 12) \leftarrow a^3\Pi_1(v = 0, J = 1)$ band. Note, that the F_2 levels of $e^3\Sigma^-$ are dark states, as they cannot be accessed from $a^3\Pi_1$ due to spin selection rule $\Delta\Sigma = 0$ (F_2 levels of $e^3\Sigma^-$ have $\Omega = |\Sigma| = 1$ character, whereas wave functions of F_1 and F_3 levels are described as superpositions of $\Omega = \Sigma = 0$ and $\Omega = |\Sigma| = 1$). Dotted lines show perturbations between $e^3\Sigma^-(v = 12)$ and $A^1\Pi_1(v = 8)$ relevant for the pumping scheme. The selection rules for the spin-orbit interaction are that interacting states have same parity and J and that $\Delta\Lambda = -\Delta\Sigma = \pm 1$. The only spin-orbit mixed rotational levels accessed in this case are ($J = 1, -$) and ($J = 2, +$), which then fluoresce to $X^1\Sigma^+(v \gg 0)$ following the selection rules $\Delta J = 0, \pm 1$ and parity selection rule $+ \leftrightarrow -$. The same selection rules also hold for (1 + 1) REMPI spectroscopy through the $A^1\Pi(v = 8)$ state (*PROBE*). Color coding consistent with Figs. 3 and 4.

The $PUMP_2$ step excites CO in the Herman bands,[54]

$$e^3\Sigma^-(v = 12) \leftarrow a^3\Pi_1(v = 0, J = 1)$$
$$\lambda_2 \sim 368\ \text{nm}, \tag{4}$$

to ro-vibrational levels that are mixed, *PERTURB* − *step*, with the $A^1\Pi_1$ state,

$$e^3\Sigma^-(v = 12) \sim A^1\Pi_1(v = 8). \tag{5}$$

The interaction between these states is well documented.[51,55,56] This mixed state naturally re-emits light both in the Herman bands as well as in the 4th-positive system. The visible fluorescence back to $a^3\Pi$, which is associated with the $e^3\Sigma^-$ character of the mixed state follows the Franck-Condon factors of the $e^3\Sigma^- \rightarrow a^3\Pi$ system, while the UV emission to $X^1\Sigma^+$ associated with the $A^1\Pi_1$ character of the mixed state follows the Franck-Condon factors for the $A^1\Pi_1 \rightarrow X^1\Sigma^+$ band. Hence, spontaneous emission from the $A^1\Pi(v = 8)$ amplitude of this mixed wave function leads efficiently to very high vibrational states of $X^1\Sigma^+$. This can be enhanced with stimulated emission in a *DUMP* step,

$$A^1\Pi_1(v = 8) \rightarrow X^1\Sigma^+(v \gg 0)$$
$$\lambda_3 \sim 234\ \text{nm}. \tag{6}$$

To probe the mixed-state character of levels accessed in this work, laser induced fluorescence (LIF) is employed using two arrangements. Specifically, Herman band emission is detected with a photomultiplier tube (PMT)/filter combination sensitive only in the visible (Hamamatsu R212 UH, 185–650 nm and a 400 nm longpass filter Thorlabs FEL0400). On the other hand, 4th-positive emission is detected with a UV sensitive PMT (Hamamatsu R7154, 160–320 nm). The (1 + 1) REMPI is used to directly probe population in high vibrational states of $X^1\Sigma^+$,

$$CO^+ + e^- \overset{h\nu}{\leftarrow} A^1\Pi_1(v = 8) \overset{h\nu}{\leftarrow} X^1\Sigma^+(v = 17, 18)$$
$$\lambda_4 \sim 234\ \text{nm} \tag{7}$$

using a fourth laser and a microchannel plate assembly (MCP-050, Tectra, two plates in chevron configuration).

Downloaded 02 Jul 2012 to 134.76.223.56. Redistribution subject to AIP license or copyright; see http://jcp.aip.org/about/rights_and_permissions

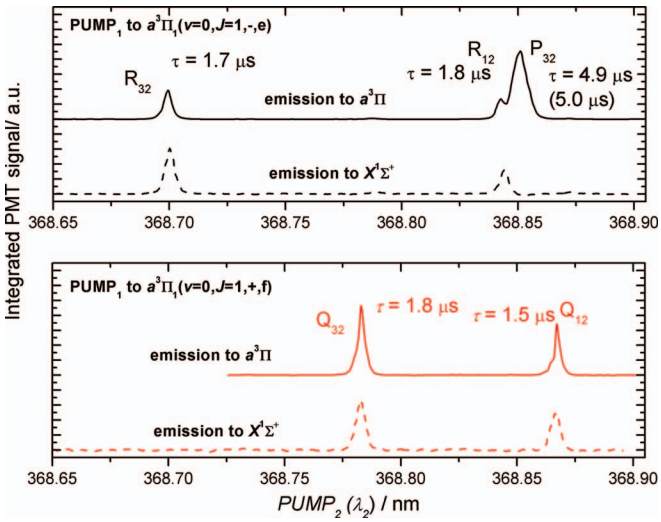

FIG. 3. $e^3\Sigma^-(v=12) \leftrightarrow A^1\Pi_1(v=8)$ spin-orbit interaction demonstrated with wavelength resolved LIF spectroscopy. Top panel shows spectra of the $e^3\Sigma^-(v=12) \leftarrow a^3\Pi_1(v=0, J=1)$ band starting in the $(-)$ parity state of $a^3\Pi_1$ and the bottom panel excitation from the corresponding $(+)$ parity state. Solid lines show red fluorescence monitoring $e^3\Sigma^- \rightarrow a^3\Pi$ emission and dashed lines show UV emission monitoring $e^3\Sigma^- \rightarrow X^1\Sigma^+$. Note, that the $P_{32}(1e)$ line only appears in the Vis-detected spectrum. This reflects the fact that $J=0$ states of $e^3\Sigma^-$ cannot mix with $A^1\Pi_1$. The mixed states also show a shorter radiative lifetime τ (values given next to the exciting transitions).

RESULTS AND DISCUSSION

The $e^3\Sigma^-(v=12)$ and the $A^1\Pi_1(v=8)$ states suffer an accidental near degeneracy at low J. This allows the finite spin-orbit interaction in the CO molecule to mix these states. This mixing can be demonstrated by LIF spectroscopy. See Fig. 3. For these spectra, CO was first prepared in either the $(-, e)$ or the $(+, f)$ parity state of $a^3\Pi_1(v'=0, J=1)$ ($PUMP_1$) and the wavelength of $PUMP_2$ (λ_2) was scanned while monitoring either (visible) Herman band (back to the $a^3\Pi_1$ state) or (UV) 4th-positive band (to the electronic ground state) fluorescence. All excitations, except $P_{32}(1, e)$, led to strong fluorescence in the 4th-positive band. This reflects one of the perturbation's selection rules, $\Delta J = 0$. The $P_{32}(1, e)$ line produces $e^3\Sigma^-(v=12, J=0)$, which cannot interact with $A^1\Pi_1$, whose lowest J state is $J=1$. Furthermore, similar LIF experiments via $e^3\Sigma^-(v=13)$, where accidental near degeneracies with the $A^1\Pi_1(v)$ are not present, showed no detectable 4th-positive band emission, reflecting the absence of singlet-triplet mixing.

To further characterize the degree of mixing, we also measured radiative lifetimes of the mixed $e^3\Sigma^-(v=12) \sim A^1\Pi_1(v=8)$ levels important for this work. The accuracy with which we could derive these lifetimes is unfortunately limited by the molecules' fly-out time from the viewing volume (1 mm^3) of the PMT optical imaging system. To improve our results we made lifetime measurements, τ_{obs}, with different molecular beam velocities, using mixtures of CO seeded in Kr (342 ms^{-1}), Ar (504 ms^{-1}) or H_2 (1446 ms^{-1}). We found that τ_{obs}^{-1} scaled linearly with the beam velocity, allowing us to extrapolate our observed lifetimes to zero beam velocity, τ. The lifetimes of the mixed states are reported in Fig. 3 and Table I and were found to be substantially shorter than the lifetime ($\tau = 4.9 \pm 0.9$ μs) of the unperturbed $e^3\Sigma^-\left(v'=12, J=0\right)$ level excited by the $P_{32}(1, e)$ transition. Lifetimes of rotational levels of $e^3\Sigma^-(v=13)$ were also close to 5 μs.

TABLE I. Lifetimes and mixing coefficients of the accessed $e^3\Sigma^-(v=12) \sim A^1\Pi_1(v=8)$ levels.

Rot. Level	τ[a] (μs) (this work)	τ_{calc}[b] (μs)	Mix. $A^1\Pi_1(v=8)$[c]
$J=1, F_3$	1.8 ± 0.3	1.9	0.0033
$J=1, F_1$	1.5 ± 0.3	1.8	0.0035
$J=2, F_3$	1.7 ± 0.3	1.8	0.0037
$J=2, F_1$	1.8 ± 0.3	2.1	0.0029
$J=0, F_3$	5.1 ± 0.9	5.0	0

[a]Experimental value from laser induced fluorescence decay extrapolated to zero beam velocity.
[b]Derived from the calculated mixing fractions of $A^1\Pi_1(v=8)$ and the lifetimes of the deperturbed states of 10 ns for $A^1\Pi$ and 5 μs for $e^3\Sigma^-$.
[c]Partial $A^1\Pi_1(v=8)$ character calculated from spectroscopically determined molecular constants. See Appendix for details. Results agree with literature.[60]

Mixed state lifetimes can also be derived from spectroscopically determined molecular constants,[57] taking into account spin-orbit interaction between $e^3\Sigma^-(v=12)$ and $A^1\Pi_1(v=8)$ and spin uncoupling within the $e^3\Sigma^-(v=12)$ state. These calculations are further described in the Appendix and results are consistent with our time resolved measurements. The calculations also yield mixing fractions, which give the partial $A^1\Pi_1(v=8)$ character of the predominantly $e^3\Sigma^-(v=12)$ levels.

Returning to more practical aspects of the P^3D method, we consider the quantum yield, ϕ_X, for spontaneous emission from the mixed states that results in population of $X^1\Sigma^+$. It can be shown that

$$\phi_X = 1 - \frac{\tau}{\tau_0} = 1 - \frac{1.8\ \mu s}{4.9\ \mu s} \approx 0.6, \tag{8}$$

where we used an averaged value of $\tau = 1.8$ μs for the mixed F_1 and F_3 states.

Despite the small mixing fractions, e.g., 0.35% fractional $A^1\Pi_1(v=8)$ character in $e^3\Sigma^-(v=12, J=1, F_1)$ (see Table I and Appendix), a much larger fraction of spontaneous emission to the $X^1\Sigma^+$ state (4th-positive band) results, compared to spin-allowed Herman band emission, which populates $a^3\Pi$. This is a simple consequence of the fact that the deperturbed lifetimes of the $A^1\Pi_1$ and the $e^3\Sigma^-$ states differ by a factor of 200, being 10 ns and 5 μs, respectively.[58]

Spectra of optically prepared population in $X^1\Sigma^+(v=17)$ are shown in Fig. 4, which presents (1 + 1) REMPI spectra via the $A^1\Pi_1(v=8) \leftarrow X^1\Sigma^+(v=17)$ band. We note in passing that although not shown, similar results were obtained for CO $X^1\Sigma^+(v=18)$. Depending on the chosen transitions for $PUMP_1$ and $PUMP_2$, spontaneous emission from the mixed states used in this work always populates two rotational lines with the same parity in $X^1\Sigma^+(v)$. In particular, excitation of $PUMP_1 = R(0)$ and $PUMP_2 = R_{32}(1, e)$ populates the rotational levels $J'' = (1, -)$ and $(3, -)$, resulting in five REMPI transitions $R(1)$, $Q(1)$, $R(3)$, $Q(3)$, and $P(3)$ (Fig. 4, panel (a)). For the convenience of the reader, these transitions are also shown in Fig. 2. Excitation of $PUMP_1$

Downloaded 02 Jul 2012 to 134.76.223.56. Redistribution subject to AIP license or copyright; see http://jcp.aip.org/about/rights_and_permissions

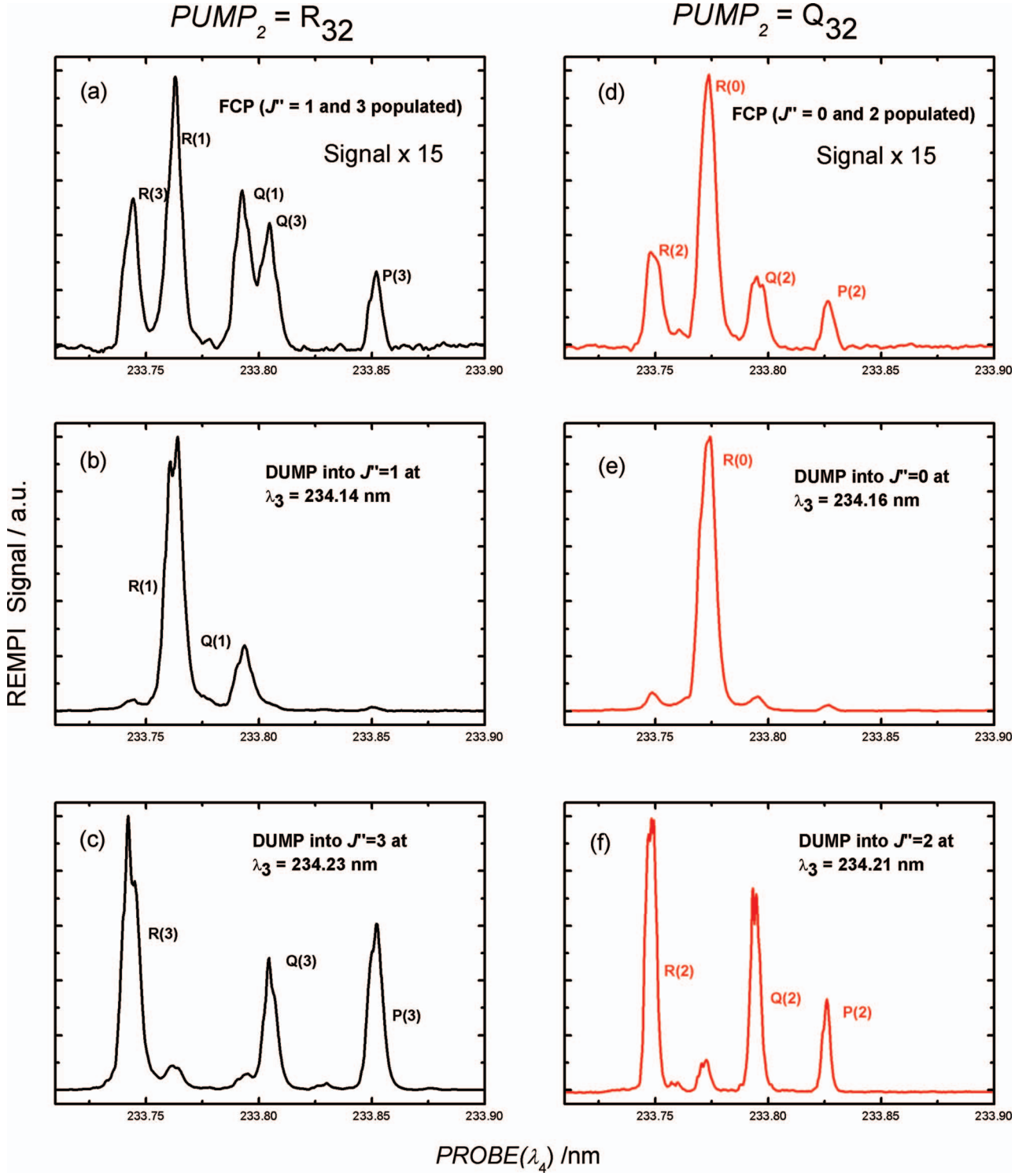

FIG. 4. Comparison of REMPI spectra of CO ($v = 17$) for different excitations in $PUMP_1$ and $PUMP_2$, with and without *DUMP*, probed by REMPI through $A^1\Pi_1(v = 8)$. An excitation of $R(0)$ by $PUMP_1$ and $R_{32}(1e)$ (compare Fig. 2) by $PUMP_2$ (panel (a)) gives rise to populations of $J'' = (1, -)$ and $(3, -)$ in CO $X^1\Sigma^+$ ($v = 17$). The REMPI spectrum a was unchanged when using the $R_{12}(1e)$ line for $PUMP_2$ instead. An excitation of $Q(1)$ in $PUMP_1$ and $Q_{32}(1f)$ (or $Q_{12}(1f)$) in $PUMP_2$ (panel (d)) results in population of $J'' = (0, +)$ and $(2, +)$ instead. Using a $DUMP(\lambda_3)$ pulse (lower four spectra) enhances the population of single ro-vibrational states by a factor of ~15 relative to spontaneous emission from the predominantly $e^3\Sigma^-$ level of the $e^3\Sigma^-(v = 12)/A^1\Pi_1(v = 8)$ pair of interacting levels. Wavelengths for the *DUMP* step are given next to the spectra. In order to achieve high population in the $J = 0$ level, which only has an $M = 0$ component, it would have been better to rotate the linear polarization of the *DUMP* laser by 90°.

$= Q(1)$ and $PUMP_2 = Q_{32}$ (1f) or $Q_{12}(1f)$ instead, populates $J'' = (0, +)$ and $(2,+)$ and four REMPI lines $R(0)$, $R(2)$, $Q(2)$, and $P(2)$ are observed (Fig. 4, panel (d)).

Population in each of these rotational levels was enhanced (up to 15 fold) by stimulated emission to a specific rotational level using a fourth (*DUMP*) laser (see panels (b), (c), (e), and (f) of Fig. 4). This population was already sufficient to observe surface scattering signals in a preliminary experiment. In this work we have produced CO in $v = 17$ and 18. Based on known Franck-Condon-factors,

Downloaded 02 Jul 2012 to 134.76.223.56. Redistribution subject to AIP license or copyright; see http://jcp.aip.org/about/rights_and_permissions

the P^3D method as described here can clearly be extended to production of CO in $v = 20$, with an internal energy of 4.7 eV.

Improvements to P^3D also appear within reach. It is significant that under these conditions, depletion of $PUMP_2$ LIF was not detected. We estimate the minimum detectable depletion to be 2%, based on past experience. As depletions greater than 25% are typically found in many SEP experiments, we estimate that a ten time improvement to the *DUMP* efficiency could be accomplished.

Equation (5) shows the singlet-triplet state mixing exploited in this work. Perturbations like this occur pairwise; hence, every perturbation involves a zeroth-order singlet mixing with a zeroth-order triplet. As the perturbation is weak, the perturbed states obtain only a small fraction of the character of their perturbing partner. In this work, we have performed SEP via the predominantly triplet member of a pair of mixed states. It might also be useful to perform SEP via the predominantly singlet member. Here, the $PUMP_2$ step – saturated with 100 μJ pulse energy in this work – would be about 100 times weaker, but the *DUMP* step could be saturated easily.

Another interesting characteristic of SEP is production of aligned and oriented samples of molecules.[48,59] Since P^3D involves several pumping steps with polarized lasers, it should also be possible to manipulate the M state distribution to obtain alignment ("helicopter" vs. "cartwheel" rotation) of the dumped molecules.

CONCLUSIONS

For the first time, CO molecules have been selectively prepared in high vibrational states ($v = 17, 18$) by means of optical pumping. For that, a pumping scheme involving two *PUMP* and one *DUMP* steps has been developed that exploits well characterized singlet-triplet interactions in the CO molecule. The production of highly vibrationally excited CO is a key step for further studies on how the dynamics of CO change when the molecule carries large amounts of internal energy.

ACKNOWLEDGMENTS

We would like to acknowledge the Alexander von Humboldt Foundation and the National Science Foundation (NSF), CHE-1058709 for the participation of R.W.F. in this work.

APPENDIX: CALCULATION OF MIXING COEFFICIENTS AND LIFETIMES OF THE $e^3\Sigma^-(v = 12)$ LEVELS INTERACTING WITH $A^1\Pi_1$

The molecular Hamiltonian used by Field *et al.*[51,61] is given by

$$H = H_{ev} + H_{SO} + H_R + H_{SS} + H_{SR},$$

where H_{ev} is the vibronic part of the Hamiltonian. H_{SO}, H_{SS}, and H_{SR} are spin-obit, spin-spin, and spin-rotation operators, respectively (the spin rotation operator H_{SR} is neglected in this calculation) and are described by Freed *et al.*[62] The rotational part of the Hamiltonian H_R is given by[63]

$$H_R = B\left(J^2 - J_z^2\right) + B\left(L^2 - L_z^2\right) + B\left(S^2 - S_z^2\right) + B(L_+S_- + L_-S_+) - B(J_+L_- + J_-L_+) - B(J_+S_- + J_-S_+),$$

where $(L^2 - L_z^2)$ is replaced by $L_\perp^2$, which is treated as a constant and ignored. The first three terms of H_R have only diagonal matrix elements. The eigenvalues of the rotational eigenvalue equation

$$B\left(J^2 - J_z^2\right) + B\left(L^2 - L_z^2\right) + B\left(S^2 - S_z^2\right) \times |JM\Omega\rangle = E^{ROT}|JM\Omega\rangle$$

are given by ($L_\perp^2$ ignored)

$$E^{ROT} = B[J(J+1) - \Omega^2 + S(S+1) - \Sigma^2].$$

The last terms of H_R have off-diagonal matrix elements that follow $\Delta\Lambda = -\Delta\Sigma = \pm 1$, $\Delta\Omega = \Delta\Lambda = \pm 1$, and $\Delta\Omega = \Delta\Sigma = \pm 1$, respectively.

Here, we study the interaction between levels of $e^3\Sigma^-(v = 12)$ and $A^1\Pi_1(v = 8)$ of the same J and parity (selection rule $\Delta J = 0$ for all pertubations). The $e^3\Sigma^-(v = 12)$ state has a total electron spin of $S = 1$ and a molecule fixed projection of the total electronic orbital angular momentum of $\Lambda = 0$. We use a Hund's case (a) basis set of the form $|S\Lambda\Sigma\rangle$ with $\Sigma = 1, 0, -1$, symmetrized with respect to reflection in a plane containing the internuclear axis.

$$\Phi_1(e^3\Sigma^-) = \frac{1}{\sqrt{2}}(|1, 0^-, 1\rangle + |1, 0^-, -1\rangle)\ (e\text{-symmetry}),$$

$$\Phi_2(e^3\Sigma^-) = |1, 0^-, 0\rangle\ (e\text{-symmetry}),$$

$$\Phi_3(e^3\Sigma^-) = \frac{1}{\sqrt{2}}(|1, 0^-, -1\rangle - |1, 0^-, 1\rangle)\ (f\text{-symmetry}).$$

These functions interact via the *S-uncoupling operator* $-B(J_+S_- + J_-S_+)$, which is responsible for heterogeneous ($\Delta\Omega = \pm 1$) electronic-rotational interaction between basis states with identical values of S and Λ, but different Σ. The matrix element connecting $\Phi_2(e^3\Sigma^-) = {}^3\Sigma_0^-(e)$ and $\Phi_1(e^3\Sigma^-) = {}^3\Sigma_1^-(e)$ is given by

$$\langle \Lambda, S, \Sigma = 0, \Omega = 0, v| - BJ_\pm S_\mp|\Lambda, S, \Sigma \pm 1, \Omega \pm 1, v'\rangle = -B_{vv'}\sqrt{S(S+1) \times J(J+1)}.$$

In addition, we include the diagonal matrix elements of the spin-spin operator, H_{SS}, which, for $\Delta S = \Delta\Sigma = 0$, is

TABLE II. Molecular constants of the Hamiltonian matrix.

	Parameter	Value (cm^{-1}) (Ref. 57)	Physical origin
$e^3\Sigma^-(v = 12)$	E_e	75583.112	Vibronic energy
	B_e	1.07159	Rotational constant
	λ	0.783[a]	Spin-spin constant
$A^1\Pi_1(v = 8)$	E_A	75632.97	Vibronic energy
	B_A	1.41567	Rotational constant
Off diagonal	A_{10}^s	−4.03	Off diagonal spin-orbit constant

[a]Calculated from $C = -0.522\ cm^{-1}$ via $C = -\frac{2}{3}\lambda$.

Downloaded 02 Jul 2012 to 134.76.223.56. Redistribution subject to AIP license or copyright; see http://jcp.aip.org/about/rights_and_permissions

TABLE III. Energy, lifetimes, and mixing coefficients for the predominantly $e^3\Sigma^-(v = 12)$ state.

		Calculation							Experimental	
Label		E (cm^{-1})	α^2	β^2	γ^2	δ^2	ε^2	τ (μs)	E [a] (cm^{-1})	τ (μs)
$J = 1$	F_3	75589.0	0.4224	0.5743	…	0.0033	…	1.88	75589.2	1.8 ± 0.3
	F_2	75585.5	…	…	0.9933	…	0.0067	1.15	…	…
	F_1	75582.9	0.5708	0.4257	…	0.0035	…	1.82	75583.0	1.5 ± 0.3
$J = 2$	F_3	75595.5	0.4537	0.5426	…	0.0037	…	1.76	75595.4	1.7 ± 0.3
	F_2	75589.8	…	…	0.9936	…	0.0064	1.20	…	…
	F_1	75585.0	0.5398	0.4573	…	0.0029	…	2.05	75584.8	1.8 ± 0.3

[a]Shifted by an offset of -5.5 cm^{-1}.

given by

$$\langle S, \Sigma|H_{SS}|S, \Sigma\rangle = \frac{2}{3}\lambda[3\Sigma^2 - S(S+1)].$$

The operators $B(L_+S_- + L_-S_+)$ and $-B(J_+L_- + J_-L_+)$ can be neglected, as the $e^3\Sigma^-(v = 12)$ state has zero electronic orbital angular momentum.

For the $A^1\Pi_1(v = 8)$ state we also use *e/f* – symmetrized basis functions of the form $|S, \Lambda, \Sigma\rangle$ given by

$$\Phi_4(A^1\Pi_1) = \frac{1}{\sqrt{2}}(|0, 1, 0\rangle + |0, -1, 0\rangle) \text{ (}e\text{-symmetry)},$$

$$\Phi_5(A^1\Pi_1) = \frac{1}{\sqrt{2}}(|0, 1, 0\rangle - |0, -1, 0\rangle) \text{ (}f\text{-symmetry)}.$$

These $A^1\Pi_1$ basis states can interact with the basis states of $e^3\Sigma^-$ via the spin-orbit term following the selection rules $\Delta\Lambda = -\Delta\Sigma = \pm 1$ and $e \nleftrightarrow f$ with the matrix element $A^s_{10} \equiv \langle {}^1\Pi_1 e/f|\mathrm{H}_{SO}|{}^3\Sigma^-_1 e/f\rangle$.

Evaluating the matrix elements in the basis of $\{\Phi_1(e^3\Sigma^-), \Phi_2(e^3\Sigma^-), \Phi_4(A^1\Pi_1)\}$ [*e*-symmetry] and $\{\Phi_3(e^3\Sigma^-), \Phi_5(A^1\Pi_1)\}$ [*f*-symmetry] results in the following Hamiltonian:

$$\begin{pmatrix}
E_e + B_e J(J+1) + \frac{2}{3}\lambda & -\sqrt{2}B_e[2J(J+1)]^{0.5} & A^s_{10} & 0 & 0 \\
-\sqrt{2}B_e[2J(J+1)]^{0.5} & E_e + B_e[J(J+1)+2] - \frac{4}{3}\lambda & 0 & 0 & 0 \\
A^s_{10} & 0 & E_A + B_A[J(J+1)-1] & 0 & 0 \\
0 & 0 & 0 & E_e + B_e J(J+1) + \frac{2}{3}\lambda & A^s_{10} \\
0 & 0 & 0 & A^s_{10} & E_A + B_A \\
 & & & & [J(J+1)-1]
\end{pmatrix}$$

The Hamiltonian factors into 3×3 [*e*-symmetry] and a 2×2 [*f*-symmetry] diagonal block in accordance with the selection rule $e \nleftrightarrow f$ for molecular interactions. The molecular constants of the Hamiltonian matrix are given in Table II. Subscripts "*e*" and "*A*" denote the electronic states $e^3\Sigma^-$ and $A^1\Pi_1$, respectively.

The calculation of the eigenvalues of the Hamiltonian gives the energies of the wave functions defined by

$$\psi_i = \alpha_i\Phi_1(e^3\Sigma^-) + \beta_i\Phi_2(e^3\Sigma^-) + \gamma_i\Phi_3(e^3\Sigma^-) + \delta_i\Phi_4(A^1\Pi_1) + \varepsilon_i\Phi_5(A^1\Pi_1).$$

The mixing coefficients α_i^2, β_i^2, γ_i^2, δ_i^2, and ε_i^2 are normalized such that $\alpha_i^2 + \beta_i^2 + \delta_i^2 = 1$ and $\gamma_i^2 + \varepsilon_i^2 = 1$.

Mixing coefficients for the predominantly $e^3\Sigma^-$ levels are given in Table III. At $J = 0$, the $A^1\Pi_1(v = 8)$ state lies $\sim$50 cm^{-1} higher in energy than the $e^3\Sigma^-(v = 12)$ state. This energy difference is large compared to the spin-orbit interaction of $A^s_{10} = -4.03$ cm^{-1}. Thus, the predominantly $e^3\Sigma^-$ levels have small $A^1\Pi_1$ character (defined by δ_i^2 or ε_i^2 as these mixing coefficients give the contribution of the $J = 2$ state to the predominantly $e^3\Sigma^-$ wave functions) and are labeled for a given J by F_3, F_2, and F_1 starting from the highest to the lowest energy corresponding to $J = N - 1, N, N + 1$.

From the mixing coefficients it is then possible to derive the lifetimes of the interacting levels. Unperturbed lifetimes of the $A^1\Pi_1$ and the $e^3\Sigma^-$ states are 10 ns and 5 μs, respectively.[58] The lifetimes of mixed states are given by

$$\frac{1}{\tau} = \frac{1 - (\delta^2 + \varepsilon^2)}{5\ \mu\text{s}} + \frac{\delta^2 + \varepsilon^2}{10\ \text{ns}}.$$

The derived lifetimes are also given in Table III. The lifetimes for F_1 and F_3 levels are very similar, which is due to the strong spin-spin interaction between $\Phi_1(e^3\Sigma^-)$. The lifetimes of the F_2 levels is expected to be shorter (1.15 μs for $J = 1$ and

Downloaded 02 Jul 2012 to 134.76.223.56. Redistribution subject to AIP license or copyright; see http://jcp.aip.org/about/rights_and_permissions

1.20 μs for $J = 2$). The F_2 levels however cannot be accessed from $a^3\Pi_1$ due to the spin selection rule, $\Delta\Sigma = 0$.

[1] D. M. Neumark, A. M. Wodtke, G. N. Robinson, C. C. Hayden, and Y. T. Lee, J. Chem. Phys. **82**(7), 3045 (1985).
[2] C. T. Rettner and D. J. Auerbach, Science **263**(5145), 365 (1994).
[3] R. D. Beck, P. Maroni, D. C. Papageorgopoulos, T. T. Dang, M. P. Schmid, and T. R. Rizzo, Science **302**(5642), 98 (2003).
[4] L. Schnieder, K. Seekamp-Rahn, F. Liedeker, H. Steuwe, and K. H. Welge, Faraday Discuss. Chem. Soc. **91**, 259 (1991).
[5] C. Kittrell, E. Abramson, J. L. Kinsey, S. A. McDonald, D. E. Reisner, R. W. Field, and D. H. Katayama, J. Chem. Phys. **75**(5), 2056 (1981).
[6] M. Silva, R. Jongma, R. W. Field, and A. M. Wodtke, Annu. Rev. Phys. Chem. **52**(1), 811 (2001).
[7] E. Abramson, R. W. Field, D. Imre, K. K. Innes, and J. L. Kinsey, J. Chem. Phys. **80**(6), 2298 (1984).
[8] D. E. Reisner, P. H. Vaccaro, C. Kittrell, R. W. Field, J. L. Kinsey, and H. L. Dai, J. Chem. Phys. **77**(1), 573 (1982).
[9] X. Yang and A. M. Wodtke, J. Chem. Phys. **92**(1), 116 (1990).
[10] X. M. Yang, E. H. Kim, and A. M. Wodtke, J. Chem. Phys. **93**(6), 4483 (1990).
[11] X. M. Yang, C. A. Rogaski, and A. M. Wodtke, J. Opt. Soc. Am. B **7**(9), 1835 (1990).
[12] X. M. Yang, C. A. Rogaski, and A. M. Wodtke, J. Chem. Phys. **92**(3), 2111 (1990).
[13] Y. S. Choi and C. B. Moore, J. Chem. Phys. **94**(8), 5414 (1991).
[14] J. C. Crane, H. Nam, H. Clauberg, H. P. Beal, I. J. Kalinovski, R. G. Shu, and C. B. Moore, J. Phys. Chem. A **102**(47), 9433 (1998).
[15] C. Beck, R. Schinke, and J. Koput, J. Chem. Phys. **112**(19), 8446 (2000).
[16] H. Ishikawa, R. W. Field, S. C. Farantos, M. Joyeux, J. Koput, C. Beck, and R. Schinke, Annual. Rev. Phys. Chem. **50**(1), 443 (1999).
[17] D. Murdock, L. A. Burns, and P. H. Vaccaro, J. Chem. Phys. **127**(8), 081101 (2007).
[18] D. Murdock, L. A. Burns, and P. H. Vaccaro, Phys. Chem. Chem. Phys. **12**(29), 8285 (2010).
[19] X. R. Chen, H. Zhao, C. H. Zhang, and L. Li, Chem. Phys. Lett. **136**(6), 546 (1987).
[20] Q. Zhang, S. A. Kandel, T. A. W. Wasserman, and P. H. Vaccaro, J. Chem. Phys. **96**(2), 1640 (1992).
[21] K. Yamanouchi, H. Yamada, and S. Tsuchiya, J. Chem. Phys. **88**(8), 4664 (1988).
[22] R. Bigwood, B. Milam, and M. Gruebele, Chem. Phys. Lett. **287**(3–4), 333 (1998).
[23] A. Geers, J. Kappert, F. Temps, and J. W. Wiebrecht, J. Opt. Soc. Am. B **7**(9), 1935 (1990).
[24] G. W. Adamson, X. S. Zhao, and R. W. Field, J. Mol. Spectrosc. **160**(1), 11 (1993).
[25] J. M. Price, J. A. Mack, C. A. Rogaski, and A. M. Wodtke, Chem. Phys. **175**(1), 83 (1993).
[26] C. A. Rogaski, J. M. Price, J. A. Mack, and A. M. Wodtke, Geophys. Res. Lett. **20**(24), 2885, doi:10.1029/93GL03149 (1993).
[27] R. W. Field and H. L. Dai, *Molecular Dynamics and Spectroscopy by Stimulated Emission Pumping*, Advanced Series in Physical Chemistry Vol. 4, (World Scientific, 1995).
[28] Y. H. Huang, C. T. Rettner, D. J. Auerbach, and A. M. Wodtke, Science **290**(5489), 111 (2000).
[29] N. H. Nahler, J. D. White, J. LaRue, D. J. Auerbach, and A. M. Wodtke, Science **321**(5893), 1191 (2008).
[30] J. D. White, J. Chen, D. Matsiev, D. J. Auerbach, and A. M. Wodtke, J. Vac. Sci. Technol. A **23**(4), 1085 (2005).
[31] J. D. White, J. Chen, D. Matsiev, D. J. Auerbach, and A. M. Wodtke, Nature (London) **433**(7025), 503 (2005).
[32] J. D. White, J. Chen, D. Matsiev, D. J. Auerbach, and A. M. Wodtke, J. Chem. Phys. **124**(6), 064702 (2006).
[33] C. Bartels, R. Cooper, D. J. Auerbach, and A. M. Wodtke, Chem. Sci. **2**(9), 1647 (2011).
[34] A. M. Wodtke, D. Matsiev, and D. J. Auerbach, Prog. Surf. Sci. **83**(3), 167 (2008).
[35] A. M. Wodtke, J. C. Tully, and D. J. Auerbach, Int. Rev. Phys. Chem. **23**(4), 513 (2004).
[36] I. Rahinov, R. Cooper, D. Matsiev, C. Bartels, D. J. Auerbach, and A. M. Wodtke, Phys. Chem. Chem. Phys. **13**(28), 12680 (2011).
[37] J. Larue, T. Schafer, D. Matsiev, L. Velarde, N. H. Nahler, D. J. Auerbach, and A. M. Wodtke, Phys. Chem. Chem. Phys. **13**(1), 97 (2011).
[38] J. L. LaRue, T. Schafer, D. Matsiev, L. Velarde, N. H. Nahler, D. J. Auerbach, and A. M. Wodtke, J. Phys. Chem. A **115**(50), 14306 (2011).
[39] R. Cooper, I. Rahinov, C. Yuan, X. M. Yang, D. J. Auerbach, and A. M. Wodtke, J. Vac. Sci. Technol. A **27**(4), 907 (2009).
[40] I. Rahinov, R. Cooper, C. Yuan, X. M. Yang, D. J. Auerbach, and A. M. Wodtke, J. Chem. Phys. **129**(21), 214708 (2008).
[41] M. Morin, N. J. Levinos, and A. L. Harris, J. Chem. Phys. **96**(5), 3950 (1992).
[42] M. Head-Gordon and J. C. Tully, J. Chem. Phys. **96**(5), 3939 (1992).
[43] H. C. Chang and G. E. Ewing, J. Phys. Chem. **94**(19), 7635 (1990).
[44] C. Flament, T. George, K. A. Meister, J. C. Tufts, J. W. Rich, V. V. Subramaniam, J. P. Martin, B. Piar, and M. Y. Perrin, Chem. Phys. **163**(2), 241 (1992).
[45] S. Wurm, P. Feulner, and D. Menzel, Phys. Rev. Lett. **74**(13), 2591 (1995).
[46] M. Eidelsberg, F. Rostas, J. Breton, and B. Thieblemont, J. Chem. Phys. **96**(8), 5585 (1992).
[47] J. D. Simmons, A. M. Bass, and S. G. Tilford, Astrophys. J. **155**(1p1), 345 (1969).
[48] D. Matsiev, J. Chen, M. Murphy, and A. M. Wodtke, J. Chem. Phys. **118**(21), 9477 (2003).
[49] J. Chen, D. Matsiev, J. D. White, M. Murphy, and A. M. Wodtke, Chem. Phys. **301**(2–3), 161 (2004).
[50] L. Velarde, D. P. Engelhart, D. Matsiev, J. LaRue, D. J. Auerbach, and A. M. Wodtke, Rev. Sci. Instrum. **81**(6), 063106 (2010).
[51] R. W. Field, S. G. Tilford, J. D. Simmons, and R. A. Howard, J. Mol. Spectrosc. **44**(2), 347 (1972).
[52] J. M. Price, A. Ludviksson, M. Nooney, M. Xu, R. M. Martin, and A. M. Wodtke, J. Chem. Phys. **96**(3), 1854 (1992).
[53] M. Drabbels, S. Stolte, and G. Meijer, Chem. Phys. Lett. **200**(1–2), 108 (1992).
[54] P. H. Krupenie, "The Band Spectrum of Carbon Monoxide," in *Natl. Stand. Ref. Data. Ser.* (Washington D.C.: Nat. Bur. Stds., 1966).
[55] F. Rostas, M. Eidelsberg, A. Jolly, J. L. Lemaire, A. Le Floch, and J. Rostas, J. Chem. Phys. **112**(10), 4591 (2000).
[56] M. Eidelsberg and F. Rostas, Astrophys. J., Suppl. Ser. **145**(1), 89 (2003).
[57] R. W. Field, "Spectroscopy and perturbation analysis in excited states of CO and CS," PhD thesis, 1972 and supplementary material.
[58] A. Lefloch, J. Rostas, and F. Rostas, Chem. Phys. **142**(2), 261 (1990).
[59] T. Schäfer, N. Bartels, N. Hocke, X. Yang, and A. M. Wodtke, Chem. Phys. Lett. **535**, 1 (2012).
[60] D. C. Morton and L. Noreau, Astrophys. J. Suppl. Ser. **95**, 301 (1994).
[61] R. W. Field and H. Lefebvre-Brion, *The Spectra and Dynamics of Diatomic Molecules*, 1st ed. (Academic, 2004).
[62] K. F. Freed, J. Chem. Phys. **45**(11), 4214 (1966).
[63] J. T. Hougen (2001), The Calculation of Rotational Energy Levels and Rotational Line Intensities in Diatomic Molecules (version 1.0). [Online] Available: http://physics.nist.gov/DiatomicCalculations [Tuesday, 22-May-2012 11:21:12 EDT]. National Institute of Standards and Technology, Gaithersburg, MD.

Downloaded 02 Jul 2012 to 134.76.223.56. Redistribution subject to AIP license or copyright; see http://jcp.aip.org/about/rights_and_permissions